Comparison of the FARO Focus^{S} 3D Laser Scanner and Manual Methods in Bloodstain Pattern Analysis

By

ELIZABETH DURAN

THESIS

Submitted in partial satisfaction of the requirements for the degree of

MASTER SCIENCE

in

Forensic Science

in the

OFFICE OF GRADUATE STUDIES

of the

UNIVERSITY OF CALIFORNIA

DAVIS

Approved:

Dr. Ralph C Aldredge, Chair

Dr. Ruth E Dickover

Toby L Gloekler, P.E.

Committee in Charge, 2022

ACKNOWLEDGEMENTS:

I would like to thank my thesis committee, friends, and family for their support and assistance throughout completion of this research project. I would like to express my gratitude to Toby L Gloekler for giving me the opportunity to work with him on this project and for taking the time assistance with experiments. I would also like to thank him for providing the FARO Scanner and software to use for this project. A special thanks to my PI Dr. Ralph C Aldredge and thesis committee member Dr. Ruth E Dickover for their valuable feedback and recommendations.

I would like to give a special thank you to Jenny Saechao for her support and for helping me brainstorm ideas as well as providing assistance with experiments.

I would like to express my appreciation and love to my family, Karan Duran, Richard Duran, Katy Tryzna, and Simon Tryzna, for their endless love, support, and encouragement throughout this process.

This project was funded by the Forensic Science Graduate Program at the University of California, Davis and Collision Reconstruction Engineers, Inc.

TABLE OF CONTENTS

1. ABSTRACT

One of the most common types of evidence forensic investigators find at violent crime scenes is blood. The many useful properties of blood can provide an abundance of information for investigators trying to interpret what happened at a crime scene. The examination and analysis of blood and bloodstain distribution at a crime scene in attempt to determine what occurred during the crime is called bloodstain pattern analysis (BPA). Extensive research on the characteristics of blood, types of bloodstains, and the use of that information for analysis at crime scenes resulted in acceptance of BPA in legal cases. An important component of deducing the sequence of events during a crime includes determining the area-of-origin (AO) of blood spatter. This in turn can approximate the location of persons involved in the crime. Interpretation of blood spatter may prove useful in confirming or refuting the sequence of events and location(s) of suspects and victims during the crime. Bloodstains comprising the impact spatter patterns often have characteristic elliptical shapes, which give insight to their angle of impact and thus the flight path of the bloodstains. The geometric convergence of the trajectories of the blood droplets flight path in an impact spatter are used to approximate the origin in 3-dimentional space. To perform this analysis at a crime scene, investigators would calculate the angle of impact on the bloodstains in a spatter patter, attach strings to them, and pull the strings back at the angle of impact of each bloodstain. This tedious process is repeated until a visible convergence is observed. This method is called the string method. This technique has been generally accepted by experts in Blood Pattern Analysis (BPA) and has successfully been admitted in courtrooms across the country, yet there are some notable disadvantages, most notably, the significant time commitment needed to place the string and document the origin. Emerging Technologies, such as the FARO 3D laser scanners and blood spatter analysis software can improve the quality of documentation of crime

scenes and expedite the process of returning the crime scene to public use. In the research, blood spatter patterns were created by striking a pool of synthetic blood with a hammer. The patterns were documented and analyzed using the traditional string method to determine the AO. The FARO Focus^{S} 3D laser scanner was used to scan the spatter pattern and then FARO Scene and FARO Zone 3D were used to calculate the AO. The two methods were compared and the accuracy and efficacy of each were discussed. Impact angles were created on various surfaces to evaluate the accuracy of calculation of impact angle manually and with FARO Zone 3D. The results concluded that the use of FARO Scene and FARO Zone 3D produced the same accuracy of AO calculations and impact angle calculations as manual calculations. The use of the FARO 3D laser scanner was a quicker method of documentation and calculations in FARO Scene and FARO Zone 3D were easier.

LIST OF ABBREVIATIONS

SWGSTAIN	Scientific Working Group for Bloodstain Pattern Analysis
BPA	Blood Pattern Analysis
AO	Area-of-origin

LIST OF FIGURES

LIST OF TABLES

2. INTRODUCTION & BACKGROUND

2.1. History of bloodstain pattern analysis

When processing crime scenes, forensic analysists will frequently encounter one of the most common biological fluids found at a crime scene: blood [1, 2, 3]. Not only can finding blood at crime scenes aid with determining a possible suspect through DNA analysis, but it can also help establish the sequence of events that led to the bloodshed during the crime. The process of analyzing and interpreting the blood found at crime scenes is called bloodstain pattern analysis (BPA) [4, 5].

BPA was a relatively disregarded field in forensic science until the first significant study of the shape, directionality, and distribution of bloodstains conducted by Dr. Edward Piotrowski in Poland in 1895 [1, 6]. Throughout the beginning of the 20th century, there were notable advancements in the theory and practice of BPA. In 1900, Dr. Paul Jererich completed a study of bloodstain patterns found at crime scenes and in 1939, Dr. Victor Balthazard published a study about blood trajectories and how this can give insight to their origin. Balthazard originally proposed that the ratio of length to width of a bloodstain is related to the impact angle and this information can aid in determination of the blood source location [1, 6]. Dr. Paul Kirk's work on the *State of Ohio v. Samuel H. Sheppard* litigation showcased BPA and how it can be used in real cases and was a turning point for blood pattern evidence used in legal proceedings. Dr. Kirk conducted a thorough analysis on this case, which he later published, and his testimony was the first to explain BPA systematically and scientifically for a legal investigation [7]. Herbert Leon MacDonell continued Dr. Kirk's efforts in the late 20th century to show the significance of bloodstain evidence and the concept of BPA [1]. As a result of the continual acceptance and

notable works published about BPA, in 2002 the Scientific Working Group for Bloodstain Pattern Analysis (SWGSTAIN) was formed to establish guidelines for the field [6].

2.2. Introduction to bloodstain pattern analysis and its use in forensics

The main purpose of BPA is to answer the questions of who was there, what caused the bloodshed, when did these events take place, where did the blood come from, and how did the bloodstains and patterns occur [1, 8]. To help answer these questions the size, shape, physical characteristics, and distribution of the bloodstains are analyzed [4, 9, 10]. The types of bloodstains found at crime scenes and their placement within the scene can assist investigators in deducing a sequence of events. There are three main categories of bloodstains: passive stains in which the flow of blood is affected only by the force of gravity to create the stain; altered stains, which result in one bloody surface contacting another surface; and projected stains, which are caused by the expulsion of blood under pressure. Several types of bloodstains can are defined in Table 1[11-14].

Table 1: SWGSTAIN bloodstain definitions [11-14].

Category	Type of Bloodstain	Definition
Passive	Drip Stain	A bloodstain formed by a free-falling drop of blood; can calculate angle of impact
	Blood pool	An accumulation of blood
Altered	Transfer	Contact between a blood-bearing surface and a second surface; ex. bloody handprint or footprint

	Swipe	A blood-bearing surface contacting another surface with an indication of motion
	Wipe	A surface moving through
Projected	Arterial	Exposure of an artery causing arterial pressure to push out spurts of blood onto surfaces
	Cast-Off	A pattern caused by a blood-bearing object releasing blood drops due to its motion
	Exhaled/Expiration	A pattern resulting from blood being expelled through air pressure from the mouth, nose, or an open wound
	Splash	The result of a volume of blood being spilled on another surface
	Impact spatter	A pattern resulting from applied force to fluid blood dispersing it through the air; forward spatter-movement of blood drops in the same direction as the applied force; backs patter-movement of blood drops in the opposite direction as the applied force

Once an investigator has inspected the bloodstains present at a crime scene, information and locations of persons or objects, and the location from which the blood originated can be used to establish what occurred during the crime. Impact spatter patterns are one of the useful bloodstain types for determining where the blood originated [15]. The focus of this study is on impact spatter patterns.

Bloodstain pattern analysts can identify impact spatter patterns by specific characteristics of the stains. When a blood source is struck by an object, the blood breaks apart into individual spherical blood drops that are projected into the air and continue a flight path until they hit a surface creating an impact spatter pattern [16, 17]. When a blood drop hits a surface, especially at an angle smaller than 90°, the resulting bloodstain is elongated forming an elliptical shape [12, 18]. The further from 90° the impact angle is, the more elliptical the stain will be (Figure 1) [19]. A formation of a tail in the direction the stain was traveling is often observed. The size of the stains in a spatter pattern can vary based on the force of the impact and the number of stains in a pattern can vary by the volume of blood originally struck [1].

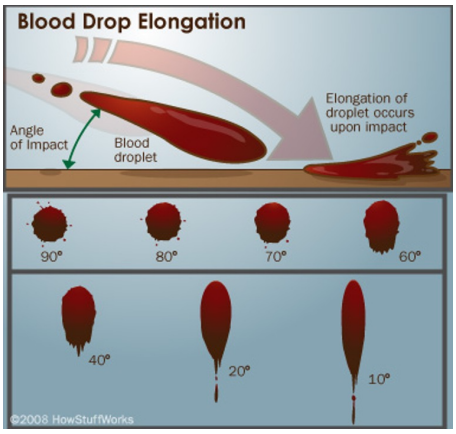

Figure 1: Diagram of blood elongation as it hits a surface and how the stain can become more elliptical as the angle of impact decreases. The tail is obvious in 10° and 30° and shows the direction the stains were traveling [19]. (reprinted with permission from HowStuffWorks)

2.3. Using impact spatter patterns to determine area of origin using the string method

One of the steps to hypothesize the sequence of events in a crime is to determine from where the blood could have originated. When investigators recognize a spatter pattern with three or more stains seemingly derived from the same impact, they can employ the manual string method to find the general area the blood in that pattern came from. This method of analysis was

developed in 1939 from Balthazard's studies about blood trajectories [8, 20]. The string method assumes a straight-line trajectory and negates the effect of gravity and wind resistance. This allows for simpler calculations while still achieving relatively precise measurements [12, 21-23]. This information assists investigators in determining the location height and orientation of the victim at the time of impact and therefore also the potential location of the perpetrator [4, 5, 12, 21, 24]. Important terminology for BPA is defined in Table 2 [1, 14, 15].

Table 2: Terminology for spatter pattern analysis [1, 14, 15]

Term	Definition
Tail	Extension of bloodstain showing directionality; may not be as visible with increase angle of impact
Spine	Narrow, elongated projections on the edge of bloodstains extending outward from the center; number of spines can increase with impact velocity [16]
Angle of Impact (α)	The angle formed between the flight path of a blood drop and the target surface the drop strikes
Area of Convergence (AOC)	Two-dimensional position of the intersection of the trajectories of bloodstains that are extended backwards at 180°
Area of Origin (AO)	Three-dimensional position in space representing the location of the blood source

The first step in calculating the AO requires selections of the stains to be used in the analysis. Careful selection of bloodstains can lead to a more accurate calculation for the AO [25]. The number of bloodstains required to determine the AO will likely differ for each case. It is

recommended to use stains with an upward trajectory and ideally with an impact angle between 10° and 30° [1, 25, 26]. Downward moving stains could have resulted in a parabolic pathway due to gravity and if used in analysis could lead to an overestimation in the height [22]. Using stains with a length between 2 mm and 10 mm and a width smaller than 4 mm is also preferred, but any stains that have a clearly defined shape are acceptable. The more distinctive the shape, the more accurate the measurement will be [22, 26].

After selecting the bloodstains to use for analysis, the impact angle is calculated using the Balthazard equation $\alpha = \arcsin\left(\frac{w}{l}\right)$, where 'α' is the impact angle (measured in degrees), 'w' is the width of the bloodstain and 'l' is the length of the bloodstain [20]. When measuring the length and width, the tail and spins are not included in the measurement [1]. An image of this idea can be seen in Figure 2 (a) [18] and (b) [19]. In the "string method" of analysis a string is pinned to the end of the bloodstain and then extended in the opposite direction that the stain was traveling at the angle of impact to be pinned on the floor. Once this is completed with all the selected bloodstains in the pattern, the distance of the blood source from the ground and two other surfaces can be measured as a three-dimensional coordinate by where all the strings approximately intersect [22, 27]. It is likely that the strings will not intersect at a single point; instead, a spherical AO will emerge. However, a single point can be estimated from the average of the intersections of strings or the estimated center of the sphere. An example of the idea behind the string method can be observed in Figure 3 [8]. This process is then repeated for all qualifying spatter at the scene.

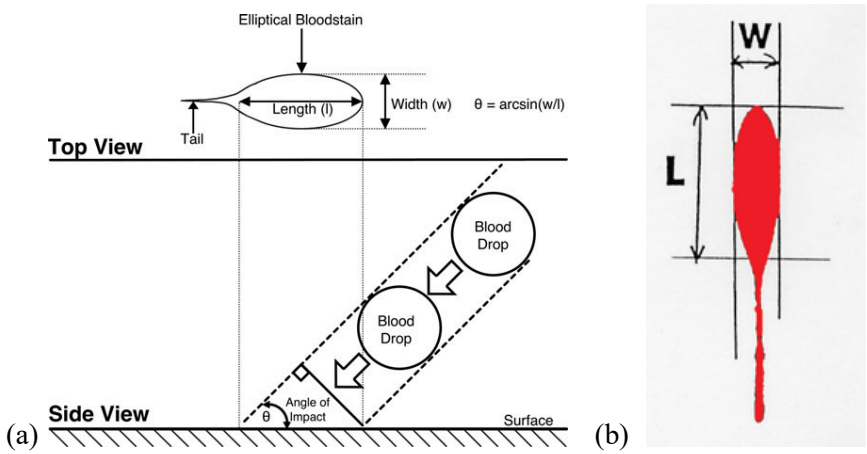

Figure 2: (a) Example of directionality (tail) in a bloodstain. Also showing the length and width measurements (top). How the angle of impact is formed when a blood drop hits a surface (bottom) [18]. (b) Shows proper measurement of the length and width for a bloodstain. The tail and spine are not included in the measurement. [19]

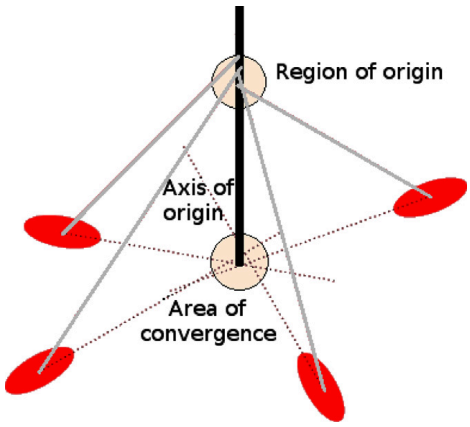

Figure 3: Diagram of how the area of convergence and area (indicated as region in the image) of origin is determined through backward trajectories of bloodstains in a spatter pattern [8].

2.4. Development of more efficient analysis methods

While the aforementioned method of BPA is a well-established approach to determine the AO, there are quicker and more efficient techniques. The process of using the string method is time consuming and destructive to the overall crime scene since the investigator must physically

attach a string to the bloodstains [18, 22]. A large number of strings are typically required to establish one AO analysis and there are often numerus blood spatter patterns to analyzed resulting in a clutter of strings throughout the scene. This method of analysis would also require a significant amount of time for blood analysts to be at the scene and could lead to contamination of other evidence. Another downside of performing the string method is errors in the precision of measurements of bloodstains by the analyst, which would result in errors in the angle of impact and therefore an incorrect estimation in the AO. Once crime scene investigators leave a scene, all the evidence is cleaned and analyst are not able to revisit the scene to correct or repeat their calculations and examination [3, 8, 18]. These complications have created desire for a quicker and more automated approach to BPA that results in a more accurate representation of the location of the AO as well as reduce the time required at the crime scene.

Advancements in computer technology offer the application of automated analysis. Some of the early developments included computerized pattern recognition in which the computer software was able to distinguish similarities and differences in patterns. However, this was more for identification of bloodstain patterns and less actual AO analysis [28].

Photogrammetry is often used by forensic scientists to reconstruct and produce 3D models of crime scenes. This process extracts three-dimensional information from multiple photographs to create a three-dimensional space. Photogrammetry permits analyst to view the crime scene after initial investigation has concluded, but still requires a considerable amount of time to capture an entire scene [29, 30]. While useful, photogrammetry is not the optimal choice for AO analysis.

Panoramic cameras were used to capture panoramic photographs of crime scenes to create a three-dimensional model. The processing of this data was time consuming due to the

need for stitching the shots together and did not always produce high quality results. The use of 360-degree cameras were more desirable since they could capture video in real time, did not require stitching, and produced higher quality results [30]. While these were practical for crime scene reconstruction, there was still a need for programs that could perform BPA.

There are automated computer programs that have been used for BPA, such as HemoSpat and BackTrack, which perform virtual stringing for AO analysis. Both HemoSpat and BackTrack software requires input of 2D photographs and manual distance measurements to create a three-dimensional space that allows for AO calculation [3, 22, 31]. The use of HemoSpat and BackTrack are a preferable alternative to the string method; however, there are limitations to these programs. Numerous measurements are still required at the scene along with a large amount of user input of bloodstain locations and other distance measurements [3].

3D laser scanners have been used in a multitude of forensic science disciplines such as collision reconstruction, bullet trajectory documentation, suspect height analysis, crime scene reconstruction, and blood pattern analysis [31, 32]. Using 3D laser scanners can reduce the time needed at crime scenes due to short scan time, can automate measurements since measurements are taken by the scanner itself, and can improved the accuracy of calculations [22, 32]. In addition, using laser scanners for documentation and analysis is less destructive than traditional methods since analysis can be performed away from the crime scene. The use of laser scanners does not replace other forms of forensic documentation, such as photography and sketching. It is still necessary to take photographs at the scene to be able to perform analysis within the scanner software [26]. Using laser scanners can also provide easier and more distinctive documentation for court presentations since it produces a virtual environment that allows jurors to see the scene altogether as well as from different perspectives [33]. Another benefit of using 3D scanner

technology is that analysts will still have a record of the crime scene and their analysis and can repeat calculations or have the opposition conduct their own analysis with the information provided [3].

2.5. FARO Focus^S 70 3D Scanner operations and its uses in bloodstain pattern analysis

When performing a scan of an area, the FARO Focus^S 70 3D Scanner works by firing an infrared laser at varying intervals 360 degrees horizontally and 305 degrees vertically. The area directly below the scanner cannot be processed due to the design of the device, which explains only scanning 305 degrees vertically [22]. The light is reflected off objects in the surroundings and back to the scanner and the time it takes the light to return determines the distance the object is from the scanner. This process is repeated millions of times during a scan which can take as little as five minutes up to an hour depending on the area being scanned and the desired resolution. All the points taken are compiled into a "point cloud," which is a 3D virtual representation of the landscape [30]. It should be noted that surfaces such as glass, mirrors, and chrome material have issues with being detected by the scanner since most of the light is reflected away [15, 32, 33]. The data obtained can then be uploaded digitally in the accompanying software that allows the scene to be viewed at various orientations and perspectives and analysis to be performed.

FARO Scene is the proprietary software that accompanies the laser scanner. An additional software called FARO Zone 3D can be purchased. Both programs are capable of performing the BPA. High-resolution photographs can be imported into both software and stitched into the point cloud. The calculations of the length and width of bloodstains are

performed within the photograph. Then the algorithm in FARO Scene/FARO Zone 3D can extrapolated the trajectories to approximate the AO within the 3D point cloud [26, 31].

The goal of this thesis is to assess the efficiency of using the FARO Focus^S 70 3D Scanner and its accompanying software FARO Scene and FARO Zone 3D in BPA, specifically to calculate the AO in comparison to the traditional manual string method. FARO Scene and FARO Zone 3D are compared to determine which software was more favorable for AO calculation. In addition, impact angles are calculated using both methods and compared to the known impact angle. The accuracy of each method as well as the advantages and disadvantages are examined. The null hypothesis was that there is no significant difference in the use of the FARO 3D scanner and the accompanying software, FARO Scene and FARO Zone 3D, for area of origin determination compared to that of the traditional string method. The alternative hypothesis was that there is a significant difference between the two methods.

3. MATERIALS AND METHODS

Blood spatter patterns were created using a hammer and analyzed to determine the point of origin using the manual string method and the FARO Focus^S 70 3D laser scanner with analysis in both FARO Scene and FARO Zone 3D. Each experiment was performed three times at different locations.

3.1. Blood Spatter Creation:

Two sheets of plywood were set up in an L-shape configuration to model walls. The blood spatter was directed at the slab labeled the North/Main wall. The other wall was labeled the East/West wall. This aided in the measurement of the blood origin. Brown packing paper was used to cover the plywood slabs for a smooth service and easy cleanup. A stand with a flat surface top was placed a random distance from the two walls and covered with brown packing paper (Figure 4). Synthetic blood (Spatter Blood purchased from Crime Scene Forensic Supply Store) was used for easy access and safety. Spatter Blood mimics the physical characteristics of human blood, such as color and viscosity, and can produce similar droplet shapes. At ambient temperature, the blood was placed in a small pool on the flat surface of the stand. The distance from the center of the blood pool to the North/Main wall and East/West wall as well as height from the ground was measured for accuracy calculations (Table 3). These measurements would theoretically represent an x, y, z coordinate where the x-value is the distance from the North/Main wall, y-value is the distance from the East/West wall, and z-value is the height from the ground. The pool of blood was struck once with a carpenter's hammer (weight 696 grams; head diameter 1.05 in; length 13.1 in) in an overhead arc to create a spatter pattern. The impact speed and force were not controlled or documented, since such information is very rarely known.

The speed and force were intentionally varied to give unique spatter patterns for each experiment to mimic real life scenarios.

Figure 4: Set up for point of origin experiments. Constructed walls covered in brown paper packaging with stand where blood is struck to create a spatter pattern. The left wall was the north/main wall, and the right was the east/west wall. From experiment number 3.

Table 3: Distance of blood source from the North wall, East/West wall, and the height from ground for each experiment.

Experiment Number	**Distance (inches)**		
	North Wall	East/West Wall	Height
1	17.30	22.80	37.70
2	20.40	24.00	31.50
3	13.88	17.63	17.75

3.2. Marking of Blood Spatter Pattern:

An adhesive tape measure was placed across the bottom of the spatter for easy reference and photograph alignment in FARO Scene and FARO Zone 3D. Zones were created using either a pencil or light-colored lumber crayon and each zone was labeled with a number. Two to three target squares were placed in each zone, which were used to assist with photograph alignment.

3.3. Photography and 3D Scans:

Photographs were taken using a Nikon D5100 digital single-lens-reflex camera, including overall and close-ups of each zone. Scans using the FARO Focus^{S} 70 3D laser scanner were taken of the entire area. The parameters (Table 4) were used for each scan and experiment. The distance between the scanner and the wall was measured for each scan (Table 5).

Table 4: FARO Focus^{S} 70 3D laser scanner parameters.

Parameters	
Resolution	1:2
Quality	3X
Number of Points	174.8 million points
Time of Scan	17.33 minutes
Distance between Points	0.110in/30ft

Table 5: Distance of scanner from the North and East/West for scans.

Experiment Number	**Scanner Distance (inches)**	
	North Wall	East/West wall
1	62.00	26.00
2 Scan #1	45.00	18.00
2 Scan #2	25.00	46.25
3 Scan #1	39.75	12.00
3 Scan #2	27.00	38.25

3.4. String Method Point of Origin Calculation:

3.4.1. Selections and Measurements of Blood Stains:

James *et al.* (2005) and Esaias *el al.* (2020) recommendations for stain selection were considered for analysis [1 26] . The length and width of the bloodstains used were measured using digital calipers. The angle of impact for each stain was then calculated using the formula:

$$Angle = \sin^{-1}\frac{width}{Length} \qquad \text{(Equation 1)}$$

3.4.2. Placement of String and Point of Origin Measurement:

A string was attached at the point of impact of the bloodstain and pulled tautly away from the wall at the appropriate angle of impact. This process was completed with multiple bloodstains until a convergence was observed. The location where the strings roughly intersected was measured as the point of origin blood.

3.5. Processing of Scans in FARO Scene:

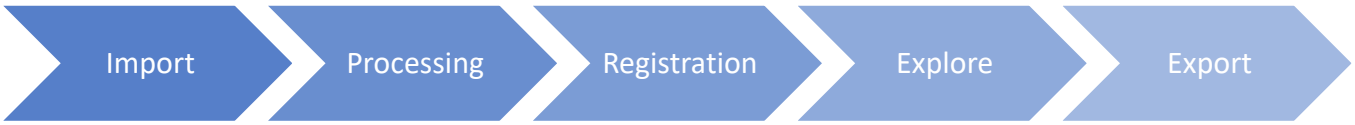

Figure 5: Schematic of scan processing using FARO Scene software

Scans are uploaded and processed in FARO Scene. The desired scan(s) are imported into Scene. Then the scan(s) are processed where color is added each scan imported and a point cloud is created [34]. Then the scans are registered which is the alignment of multiple scans using

common points between the scans [35]. Once the processing and registration steps are complete, the scan can be viewed in the explore section where it can be cropped to remove portions of the scan that are unnecessary for analysis. The point of origin calculation can be completed in this section as well as other analyses. The scan can be exported into varies file types, such as an E57, to be used in other software or exported to Zone 3D. A general overview of how scans are uploaded and processed in FARO Scene is shown in Figure 5.

3.6. 3D Point of Origin Calculation:

3.6.1. FARO Scene:

Once the scan has been processed and registered, the scan was viewed under the Explore tab to complete the point of origin calculation. The scan was put into planar view from 3D view to create virtual planes using the rectangle feature on the North wall, East/West wall, and the ground. The planes helped align a photograph on the North wall and aid with measurements. A photograph was imported into Scene to align with the scan. The plane on the North wall was selected along with the chosen photograph to pick associating points. At least six points were needed for alignment while eight were suggested for stronger alignment [36]. Eight corresponding points were selected for each experiment.

After the photograph was aligned, the ‘Forensic Wizard’ application was used to find the point of origin by selecting ‘Calculate Blood Spatter Origin.’ Drops were created using the ellipse tool to create ellipses around selected bloodstains (Figure 6). A random number of bloodstains were used to complete the analysis. After all desired bloodstain drops were created, the point of origin was generated. The scan with the aligned photograph are changed to 3D view

and the point of origin was displayed as a spiked sphere (Figure 7). The distance was measured using the ‘measure objects’ tool and by selecting the plane on the wall or ground and then the origin sphere [36]. This measured the distance in 3D.

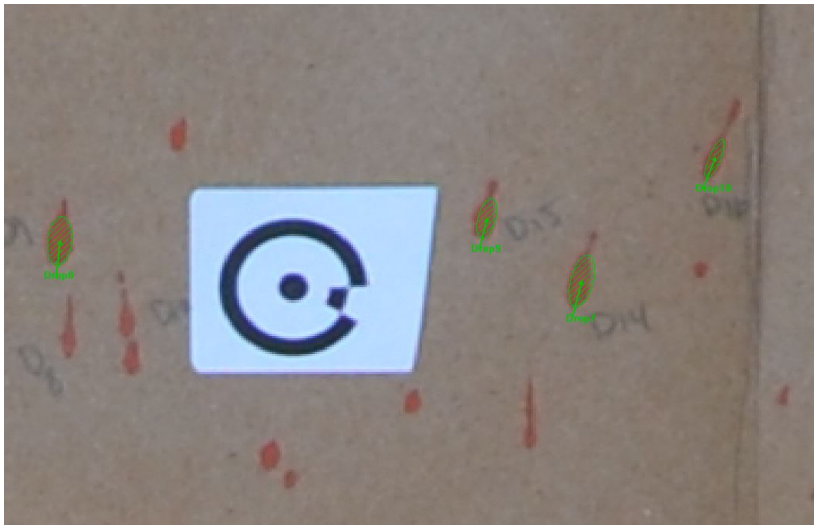

Figure 6: Ellipses created around bloodstains to create drops in FARO Scene. Green ellipse shows the drop and the arrow in the center shows direction of travel. From experiment 3 analysis.

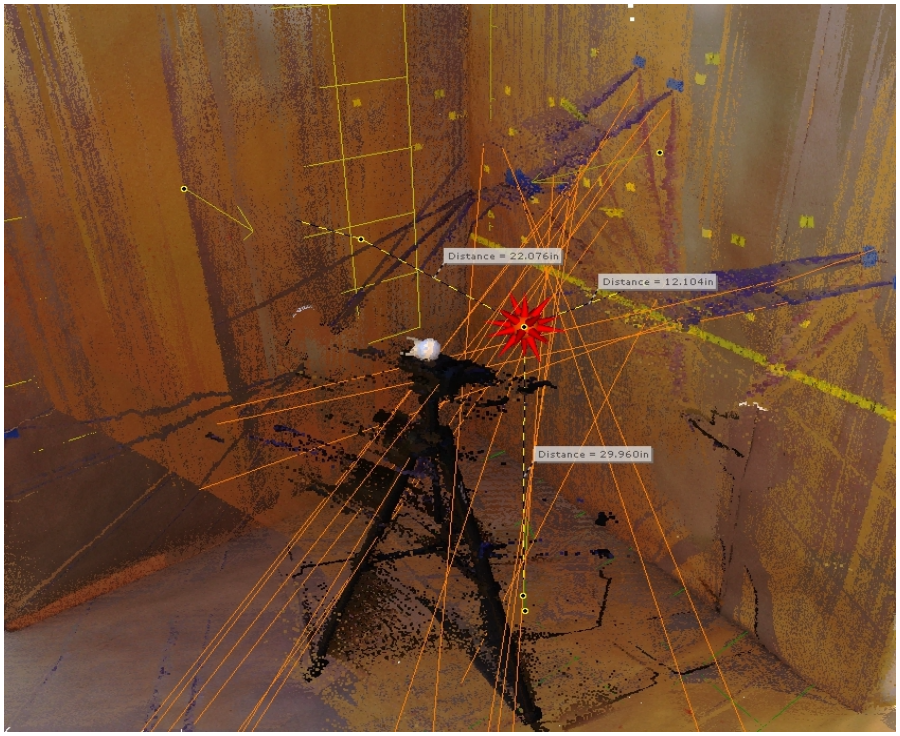

Figure 7: Point of origin calculation using (red spiked sphere) FARO Scene. Orange lines represent trajectory pathway. Distance labels from each wall and the height from the ground to the point of origin are shown. Plane on East/West wall can be seen by the yellow arrow and partial yellow grid. Tripod with foam sphere (which represented the area of origin) was placed before scan was taken. From experiment 2 analysis.

3.6.2. FARO Zone 3D

Scans were exported from FARO Scene directly to FARO Zone 3D. In FARO Zone 3D, the scan is placed on a grid. Measurements are made from the origin point at (0,0,0). The origin point was manually set at the bottom corner where the North wall and East/West wall meet. Under the 'Power Tools' section, 'Blood Spatter' was used to complete the point of origin analysis. A photograph was selected and the "Align in 2D" tool was used to align the photograph with the scan. Two corresponding points that were relatively horizontal were selected on the photo and the scan. Once complete, the photo aligned with the scan and could be micro adjusted if needed.

Droplets were created using 'edit droplets' and creating ellipses around bloodstains used for analysis (Figure 8). As each droplet was created, a trajectory pathway and point of origin, represented as a red sphere, was created in real time (Figure 9). This process could be repeated with additional photos that will be added to the point of origin calculation. The point of origin (red sphere) was selected to produce a report giving its location in space in reference to the origin point.

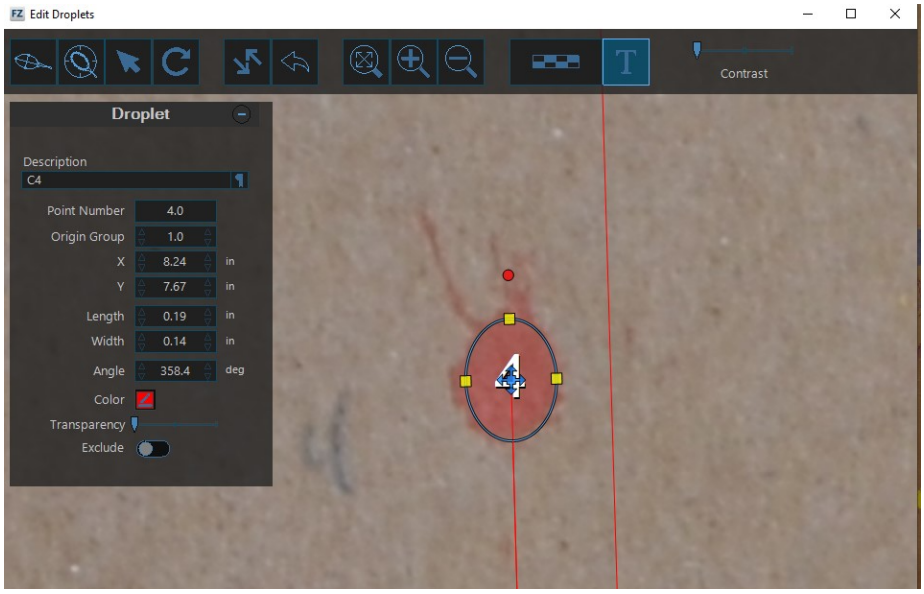

Figure 8: Ellipse created around bloodstain in FARO Zone 3D. Red line indicates trajectory line. From experiment 1 analysis.

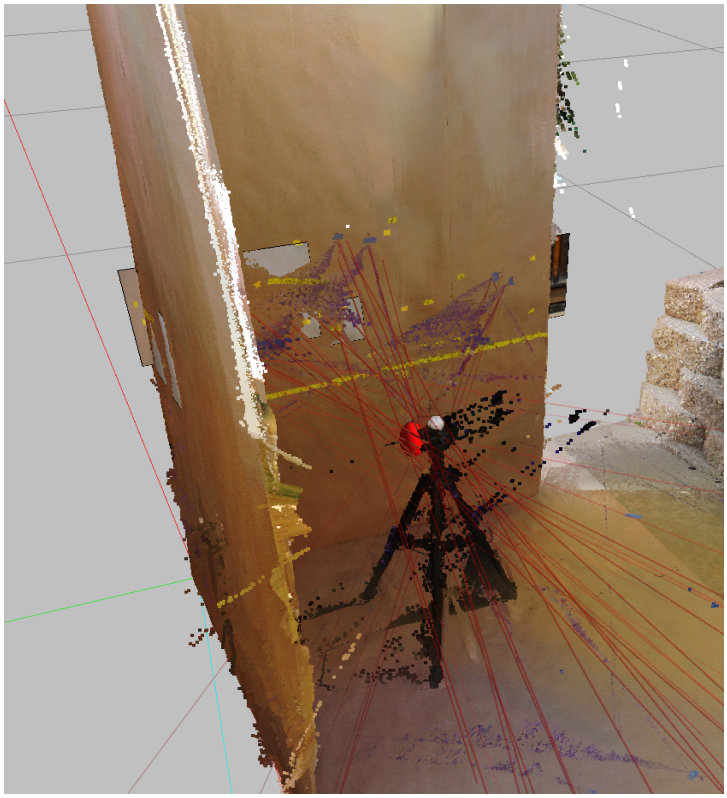

Figure 9: Point of origin calculation in FARO Zone 3D (red sphere). Red lines represent trajectory pathway. The red, green and blue line represent the X, Y, and Z axes respectively. Tripod with foam sphere (which represented the area of origin) was placed before scan was taken. From experiment 2 analysis.

3.7. Impact angle creation

Blood was dropped from a fixed height of 3 feet on various materials at known, varying angles measured using a smart level (Figure 10). The materials used were drywall, ceramic, hardwood, and a cotton T-shirt with angles from 10° to 90° randomly assigned to a letter A-I. Photographs of were taken of each angle and material. The length and width of the blood drops were measured manually and using the FARO Zone 3D software. Photographs were imported into FARO Zone 3D for analysis. From the length and width measurements, the angle was calculated and then compared to the known angle.

Figure 10: Set up for impact angles analysis.

3.8. Statistical Analysis

The absolute error and the percent error were calculated for each distance measurement (from the North (x-value), East/West (y-value), and height (z-value)) in all the point of origin

experiments. The difference between the actual and calculated distances was observed. The absolute and percent error was also calculated for the calculated angles in the known angle experiments.

4. RESULTS

4.1. Point of Origin Measurements using the string method

The calculated distances from the North Wall, East/West Wall, and the height by use of the string method are shown for each experiment (Table 6). These measurements represented the AO with the North wall, East/West wall, and the height measurements representing the x, y, and z- coordinate values respectively. The area of origins calculated by the string method are: (17.00, 25.50, 41.50) for experiment 1, (20.00, 21.50, 31.20) for experiment 2, and (11.75, 17.25, 26.0) for experiment 3.

Table 6: Measured point of origin from the string method

Experiment Number	**Distance (inches)**		
	North Wall	East/West Wall	Height
1	17.00	25.50	41.50
2	20.00	21.50	31.20
3	11.75	17.25	26.00

The absolute error and percent error were calculated for each distance value in all experiments (Table 7). The percent errors range from 0.95% to 46.48%. The largest percent error occurred for the height measurement in experiment 3 at 46.48%. The height measurements had the average greatest percent error at 19.17% The average percent error for The North wall and East/West wall measurements were 6.34% and 8.13% respectively. The average percent errors were calculated in Microsoft Excel. The height measurement for experiment 2 had the lowest error. The average percent error for all measurement was 11.21%.

Table 7: Calculated absolute error and percent error from the string method

Experiment Number	Measured Value	Measured Distance (in)	Actual Distance (in)	Absolute Error	Percent Error (%)
1	North Wall	17.00	17.30	0.30	1.73
1	East/West Wall	25.50	22.80	2.70	11.84
1	Height	41.50	37.70	3.80	10.08
2	North Wall	20.00	20.40	0.40	1.96
2	East/West Wall	21.50	24.00	2.50	10.42
2	Height	31.20	31.50	0.30	0.95
3	North Wall	11.75	13.88	2.13	15.32
3	East/West Wall	17.25	17.63	0.38	2.13
3	Height	26.00	17.75	8.25	46.48

The differences between the actual distance and the calculated distance from the string method were determined in the three experiments for each value (Figure 11). Negative values represented calculated measurements below the actual and positive values represented calculated measurements above the actual. The North wall differences ranged between -2.13 in to -0.30 in. The East/west difference ranged from -0.38 in to 2.70 in. The differences in height range from -0.30 in to 8.25 in. All difference values except that for the height in experiment 3 were below the recommended boundary for AO interpretation of less than a 20 cm (~7.87 in) difference between the actual and known measurement [18, 25].

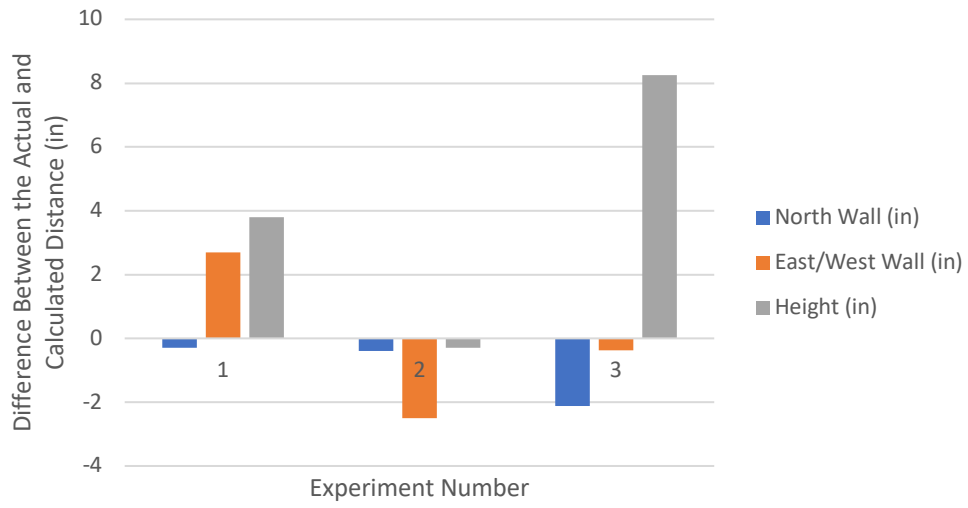

Figure 11: Difference in the actual distance and the calculated distance from the North Wall, East/West Wall, and the height from the ground from analysis using the string method.

The overall time it took to complete the string method calculations for AO was between one and a half to two hours. This included selecting bloodstains, measuring the length and width of the bloodstains, calculating the impact angle, attaching strings to all the bloodstains for the trajectory determination, and measuring the AO distances.

4.2. Point of Origin Measurements using FARO Scene

The calculated distances from the North Wall, East/West Wall, and the height performed in FARO Scene are shown for each experiment (Table 8). These measurements represented the AO. The area of origins calculated in FARO Scene are: (7.43, 19.14, 43.07) for experiment 1, (12.10, 22.08, 29.96) for experiment 2, and (7.20, 17.20, 24.45) for experiment 3.

Table 8: Measured point of origin from FARO Scene

Experiment Number	Distance (inches)		
	North Wall	East/West Wall	Height
1	7.43	19.14	43.07
2	12.10	22.08	29.96
3	7.20	17.20	24.45

The absolute error and percent error were calculated for each distance value in all experiments (Table 9). The percent errors range from 2.41% to 57.06%, where the largest percent errors occurred for the North wall measurements for all experiments with the percent error in height for experiment 3 as the next highest. The North wall measurements had the greatest average percent error at 48.60% The average percent error for East/West wall and height measurements were 8.83% and 18.96% respectively. The East/West wall measurement for experiment 3 had the lowest error of 2.41%. The average percent error for all measurement was 25.46%.

Table 9: Calculated absolute error and percent error from FARO Scene

Experiment Number	Measured Value	Measured Distance (in)	Actual Distance (in)	Absolute Error	Percent Error (%)
1	North Wall	7.43	17.30	9.87	57.06
1	East/West Wall	19.14	22.80	3.66	16.05
1	Height	43.07	37.70	5.37	14.24
2	North Wall	12.10	20.40	8.30	40.67
2	East/West Wall	22.08	24.00	1.92	8.02
2	Height	29.96	31.50	1.54	4.89
3	North Wall	7.20	13.88	6.67	48.08
3	East/West Wall	17.20	17.63	0.43	2.41
3	Height	24.45	17.75	6.70	37.76

The differences between the actual distance and the calculated distance calculated in FARO Scene were determined for the three experiments for each value (Figure 12). The North wall differences ranged between -9.87 in to -6.67 in. The East/west difference ranged from -3.66 in to -0.43 in. The differences in height range from -1.54 in to 6.70 in. The differences in the North wall for experiments 1 and 2 were the only differences above the recommended boundary of less than a 20 cm (~7.87 in) difference between the actual and calculated distance [18, 25].

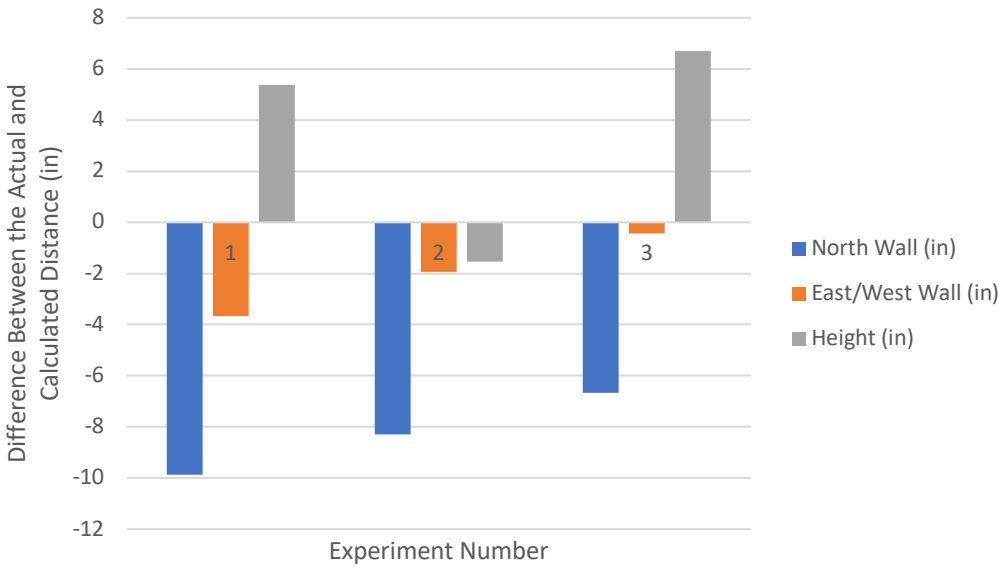

Figure 12: Difference in the actual distance and the calculated distance from the North Wall, East/West Wall, and the height from the ground from analysis using FARO Scene.

4.3. Point of Origin Measurements using FARO Zone 3D

The calculated distances from the North Wall, East/West Wall, and the height performed in FARO Zone 3D are shown for each experiment (Table 10). These measurements represented the AO. The area of origins calculated in FARO Zone 3D are: (9.36, 20.40, 39.84) for experiment 1, (18.38, 21.72, 29.28) for experiment 2, and (10.80, 17.16, 21.48) for experiment 3.

Table 10: Measured point of origin from FARO Zone 3D

Experiment Number	Distance (inches)		
	North Wall	West/East Wall	Height
1	9.36	20.40	39.84
2	18.36	21.72	29.28
3	10.80	17.16	21.48

The absolute error and percent error were calculated for each distance value in all experiments (Table 11). The percent errors range from 2.64% to 45.90% The largest error occurred for the North wall measurement in experiment 1. The North wall measurements had the greatest average percent error at 26.02% The average percent error for East/West wall and height measurements were 7.55% and 11.25% respectively. The East/West wall measurement for experiment 3 had the lowest error of 2.64%. The average percent error for all measurement was 14.94%.

Table 11: Calculated absolute error and percent error from FARO Zone 3D

Experiment Number	Measured Value	Measured Distance (in)	Actual Distance (in)	Absolute Error	Percent Error (%)
1	North Wall	9.30	17.30	7.94	45.90
1	East/West Wall	20.40	22.80	2.40	10.53
1	Height	39.84	37.70	2.14	5.68
2	North Wall	18.36	20.40	2.04	10.00
2	East/West Wall	21.72	24.00	2.28	9.50
2	Height	29.28	31.50	2.22	7.05
3	North Wall	10.80	13.88	3.08	22.16
3	East/West Wall	17.16	17.63	0.47	2.64
3	Height	21.48	17.75	3.73	21.01

The differences between the actual distance and the calculated distance calculated in FARO Zone 3D were determined for the three experiments for each value (Figure 13). The North

wall differences ranged between -7.94 in to -2.04 in. The East/west difference ranged from -2.40 in to -0.47 in. The differences in height range from -2.22 in to 3.73 in. All values were below the recommended boundary of less than a 20 cm (~7.87 in) difference between the actual and calculated distance [18, 25]. The North wall difference in experiment 1 was slightly over at a difference of 7.94 in.

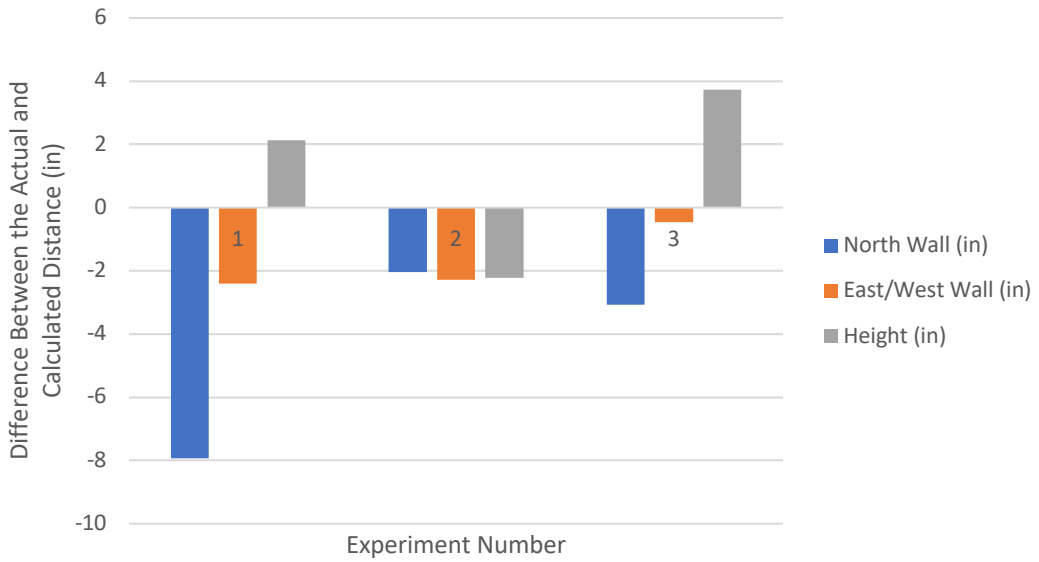

Figure 13: Difference in the actual distance and the calculated distance from the North Wall, East/West Wall, and the height from analysis using FARO Zone 3D.

The time needed for AO analysis in either FARO Scene or FARO Zone 3D took roughly 40 minutes to complete. The included uploading the scans to the software, processing the scans, uploading photographs, formation of ellipses around bloodstains, and finding the AO. The scans took just over 17 minutes to complete.

4.4. Comparison in the calculation of impact angle between manual and within FARO Zone 3D

The blood drops were most challenging to discern on the hardwood and the t-shirt. The blood drops were clearest on the drywall and ceramic. The blood was absorbed into the drywall

and t-shirt but pooled on/spilled off the ceramic and ricocheted off the hardwood. The photographs were taken in direct sunlight (Figure 14).

(a) 

(b) 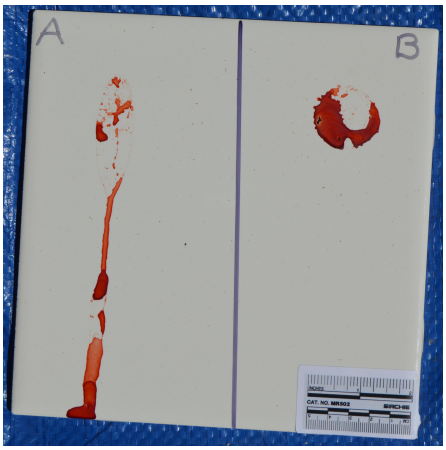

(c) 

(d) 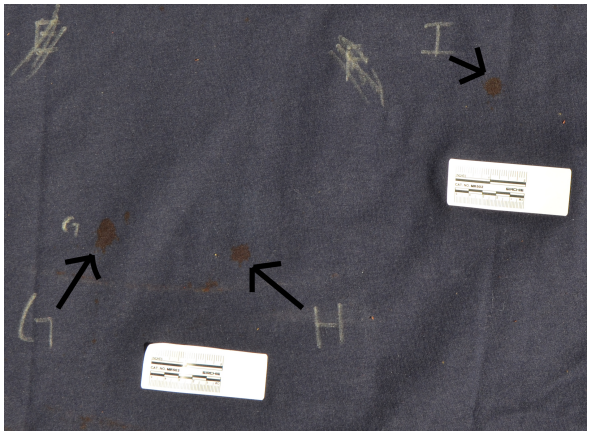

Figure 14: : Examples of several blood drops on the materials used for impact angle calculations. Letters in silver indicate the angle. (a) Blood drops of angles of 10° (E) and 80° (F) on drywall sample. Clear ellipses can be observed. (b) Blood drops of angles 20° (A) and 80° (B) on ceramic sample. Elliptical outline can be seen but blood spilled from the non-porous ceramic material. (c) Blood drops of angles 80° (A), 40° (B), and 50° (C) on hardwood sample. (d) Blood drops of angles 40° (G), 80° (H), and 70° (I) on cotton t-shirt. Black arrows point to corresponding bloodstain.

After blood drops were produced on the materials, the impact angles were calculated using Equation 1 with hand measurements and with measurements takin in FARO Zone 3D. The absolute error and percent error of the angle calculations manually and in FARO Zone 3D were determined for all angles on every material (Table 12). The highest percent error was for the T-

shirt at 10° for both methods. The calculated impact angle on the hardwood had the highest overall error while the ceramic had the lowest overall error for both methods. There were not considerable differences in the calculations of impact angles between manual and with FARO Zone 3D.

Table 12: Calculated angle using the standard method and FARO Zone 3D compared to the known angle along with the absolute and percent error

		Manual			FARO Zone 3D			
Material	Letter	Calculated Angle (°)	Absolute Error	Percent Error (%)	Calculated Angle (°)	Absolute Error	Percent Error (%)	Actual Angle (°)
Drywall	A	77.16	7.16	10.23	75.67	5.67	8.10	70
	B	15.64	14.36	47.88	14.91	15.09	50.31	30
	C	45.84	14.16	23.60	47.79	12.21	20.35	60
	D	34.26	5.74	14.35	34.43	5.57	13.93	40
	E	10.69	0.69	6.85	10.25	0.25	2.46	10
	F	80.59	0.59	0.74	77.51	2.49	3.11	80
	G	65.93	15.93	31.86	55.58	5.58	11.17	50
	H	90.00	0.00	0.00	84.95	5.05	5.62	90
	I	16.91	3.09	15.44	14.96	5.04	25.22	20
Average			6.86	16.77		6.33	15.58	
Ceramic	A	18.87	1.13	5.64	17.59	2.41	12.05	20
	B	78.16	1.84	2.30	70.98	9.02	11.27	80
	C	25.58	4.42	14.72	23.22	6.78	22.58	30
	D	57.03	12.97	18.53	43.78	26.22	37.45	70
	E	39.74	0.26	0.64	38.27	1.73	4.33	40
	F	9.76	0.24	2.42	9.37	0.63	6.32	10
	G	44.43	5.57	11.15	48.42	1.58	3.16	50
	H	90.00	0.00	0.00	88.01	1.99	2.21	90
	I	64.91	4.91	8.19	64.55	4.55	7.59	60
Average			3.48	7.07		6.10	11.88	
Hard-wood	A	63.47	16.53	20.66	67.44	12.56	15.69	80

	B	49.88	9.88	24.70	22.65	17.35	43.37	40
	C	54.90	4.90	9.81	42.27	7.73	15.45	50
	D	13.70	3.70	37.00	12.06	2.06	20.57	10
	E	65.38	24.62	27.36	71.60	18.40	20.44	90
	F	65.38	5.38	8.967	56.53	3.47	5.785	60
	G	23.58	3.58	17.89	27.47	7.47	37.37	20
	H	47.66	22.34	31.92	47.17	22.83	32.61	70
	I	20.92	9.08	30.25	15.98	14.02	46.73	30
Average			11.11	23.17		11.76	26.45	
T-Shirt	A	20.49	0.49	2.44	17.39	2.61	13.06	20
	B	65.38	15.38	30.76	67.79	17.79	35.58	50
	C	32.58	2.58	8.60	30.98	0.98	3.27	30
	D	56.44	33.56	37.29	57.00	33.00	36.67	90
	E	15.35	5.35	53.49	17.46	7.46	74.64	10
	F	54.90	5.10	8.49	74.83	14.83	24.72	60
	G	42.73	2.73	6.83	37.48	2.52	6.29	40
	H	58.21	21.79	27.24	88.22	8.22	10.28	80
	I	54.90	15.10	21.57	67.16	2.84	4.05	70
Average			11.34	21.86		10.03	23.17	

5. DISCUSSION

3D laser scanners have been a valuable tool for bloodstain pattern analysts to assist with automation of calculations and efficiency in forensic investigations. Laser scanners are advantageous to investigations in that they limit time at crime scenes and the accompanying computer software helps improve accuracy of AO measurements through computerized calculations. The FARO Focus 3D scanner has been used to document mock crime scenes and FARO Scene and Zone 3D have been used for AO determination [15, 18, 25, 33]. This study confirms that the use of the FARO Focus^{S} 70 3D scanner is an adequate documentation and analysis tool for BPA.

The results of using the traditional string method to calculate the AO were compared to analysis with FARO Scene and FARO Zone 3D from scans obtained by the FARO Focus^{S} 70 3D scanner. The average percent errors of distance calculations between calculations using the string method (11.21%) and FARO Zone 3D (14.94%) were relatively similar while the average errors for data obtained in FARO Scene was somewhat higher (25.46%). 8 out of the 9 error measurements from the string method analysis were within the recommended maximum difference of 20 cm (~7.87 in). For analysis using FARO Scene, 7 out of the 9 were below the recommended maximum difference. And for FARO Scene, all measurements were within the maximum difference [18, 25]. Performing AO analysis calculations in FARO Scene led to a higher overall error than calculations in FARO Zone 3D. It has been suggested that using FARO Zone 3D can produces better and easier to obtain results [33] Overall, there wasn't a considerable difference in the calculation of area of origin between using the string method and that of the FARO software.

When comparing the calculation of impact angle, there was not a significant difference between manual measurements and those taken in FARO Zone 3D. The average errors between the two methods were within 5% for all materials. There were some outliers for both methods, most notably for the calculation on the Drywall for sample B (30°). An error could have occurred in angle formation. Each method had higher errors in calculation of impact angle on the hardwood and t-shirt. The outlines of the bloodstains were challenging to discern on these materials due to the darker color. On the hardwood, the blood did not form clear elliptical shapes due to the texture of the hardwood, which caused the blood to be reflected off the surface. Calculating the angle of impact manually and in FARO Zone 3D is adequate for BPA.

There are variables to consider that could have influenced the results. The theory behind the string method and the operating system in FARO Scene and Zone 3D assumes a straight-line trajectory of bloodstains in an impact spatter. This, however, is not true since gravitational forces act on the blood drops as they fly through the air. Due to the effects of gravity and air resistance, the flight path of bloodstains would be closer to parabolic. These variables tend to lead to a higher estimation in height which was observed in experiments 1 and 3 for calculations with all three methods [8, 10, 20, 23, 31]. If outdoors, as these experiments were, weather could be a factor in the blood drop flight path causing errors in measurements and calculations. These variables could explain some of the higher errors in AO calculation.

It has also been noted in literature that the further from the wall the initial blood source is, the higher the error [6, 16, 21, 33]. In studies conducted by Le and Liscio, it was found that at distances 50 cm (~ 19.69 in) and 75 cm (~29.53 in) from the target wall, there is a noticeable change in error and the error was even larger at 100 cm (~39.37 in) [33]. These were most notable in the height measurement (z-value) and the measurement from the target wall (x-value).

The over estimations in height were observed in this study. As the blood source moves away from the target surface, it is also more likely that the flight path is parabolic [23]. Studies have shown that even the slightest change in the impact angle could have an effect on the x-value measurement, which is the distance from the blood source to the target surface/wall. Change in the impact angle could cause the estimation of the AO to be closer to the target wall (a smaller x-value) [16, 24].This was observed in all experiments with all methods of analysis and could account for the errors calculated.

The AO calculated in FARO Scene and FARO Zone could have resulted in lower observed accuracy due to the expertise level needed to operate the software. Photo alignment into the scan is important for accurate measurements. This requires photographs to be taken perpendicular to the wall photographed. This could have caused some slight errors in photo alignment leading to errors in calculating of AO. These errors can be improved with thorough training on operations of the software.

While the results suggest that there is not a difference in AO calculations between the string method and the FARO software, there are other variables to consider which method is preferable for BPA. The most notable consideration is that using the FARO laser scanner for documentation took significantly less time to complete (17.33 minutes). Calculations using FARO Scene or Zone 3D took under one hour to complete while analysis using the manual string method took at least one and a half hours and up to two hours to complete. Therefore, the time taken at the scene using a 3D Scanner would take half the time needed for analysis using the string method. Calculations using the FARO software also limits interaction with the scene and consequently decreases the chance of contamination.

Due to the similarities in calculations between manually using the string method and using FARO software, both methods are adequate for BPA and AO determination. However, when considering the potential for contamination, using the FARO Focus^{S} 3D laser scanner is a more suitable substitute for the lengthy string method.

6. CONCLUSION

The string method has been a practical way to determine the AO when performing BPA to aid analysts in deducing a possible sequence of events of violent crimes. This method involves measuring impact angles of bloodstains in an impact spatter pattern and using strings to show trajectories which lead to an area of convergence representing the possible blood origin. This can then help determine locations of persons involved in the crime [1, 6, 12]. While this method has been shown to be adequate in estimation of the AO, there was a need for a more efficient method that limited time at crime scenes, reduced the chances of contaminations, and allowed for analysis away from the crime scene [3, 18, 20, 22]. Application of 3D laser scanners have been shown to improve ease and accuracy of documentation and calculations [18, 20, 26, 28]. This study confirmed that the FARO Focus^{S} 3D laser scanner was allowed for quicker and easier documentation. However, the accuracy of calculations in the FARO software was discovered to be equal to that of the string method for AO calculations and determination of angle of impact. Nevertheless, it is recommended to use the FARO 3D laser scanner for AO determination and BPA due to the disadvantages of the string method, mainly in the regard of time and potential contamination of evidence.

Further evaluation could be beneficial to advance the use and acceptance of 3D laser technology for BPA. Additional experiments could be performed using other blunt objects and various surfaces to confirm results and to continue examination of the effectiveness of the FARO 3D scanner. Further research may include studies examining the use of cast-off stains in BPA and AO estimation to give more information about what could have potentially happened based on locations of persons. Some preliminary studies of cast-off stains have been conducted by Liscio et al. [37]. While challenging, trying to incorporate parabolic flight for AO calculations

could be attempted. There are other 3D scanners and software, such as Leica, that are available for analysis and studies on the advantages, disadvantages and accuracy could be valuable for future studies [38].

7. REFERENCES

1. James SH, Kish PE, Sutton TP. Principles of Bloodstain Pattern Analysis. :574.

2. Arthur RM, Humburg PJ, Hoogenboom J, Baiker M, Taylor MC, de Bruin KG. An image-processing methodology for extracting bloodstain pattern features. Forensic Sci Int 2017;277:122–3.

3. Joris P, Develter W, Jenar E, Suetens P, Vandermeulen D, Van de Voorde W, et al. HemoVision: An automated and virtual approach to bloodstain pattern analysis. Forensic Sci Int 2015;251:116–23.

4. Flight C, Jones M, Ballantyne KN. Determination of the maximum distance blood spatter travels from a vertical impact. Forensic Sci Int 2018;293:27–36.

5. de Bruin KG, Stoel RD, Limborgh JCM. Improving the Point of Origin Determination in Bloodstain Pattern Analysis. J Forensic Sci 2011;56(6):1476–82.

6. Gardner RM, Bevel T. Bloodstain Pattern Analysis with an Introduction to Crime Scene Reconstruction. :440.

7. Bloodstain Pattern Analysis. Forensic Evidence in Court. Chichester, UK: John Wiley & Sons, Ltd, 2016;277–92.

8. Vitiello A, Di Nunzio C, Garofano L, Saliva M, Ricci P, Acampora G. Bloodstain pattern analysis as optimisation problem. Forensic Sci Int 2016;266:e79–85.

9. Lee S-Y, Seo Y-I, Moon B-S, Kim J-P, Goh J-M, Park N-K, et al. Study on development of forensic blood substitute: Focusing on bloodstain pattern analysis. Forensic Sci Int 2020;316:110461.

10. Laan N, de Bruin KG, Slenter D, Wilhelm J, Jermy M, Bonn D. Bloodstain Pattern Analysis: implementation of a fluid dynamic model for position determination of victims. Sci Rep 2015;5(1):11461.

11. Attinger D, Moore C, Donaldson A, Jafari A, Stone HA. Fluid dynamics topics in bloodstain pattern analysis: Comparative review and research opportunities. Forensic Sci Int 2013;231(1–3):375–96.

12. Peschel O, Kunz SN, Rothschild MA, Mützel E. Blood stain pattern analysis. Forensic Sci Med Pathol 2011;7(3):257–70.

13. FBI — Standards and Guidelines - Scientific Working Group on Bloodstain Pattern Analysis: Recommended Terminology - April 2009. https://archives.fbi.gov/archives/about-us/lab/forensic-science-communications/fsc/april2009/standards/2009_04_standards01.htm

14. Choromanski K. Bloodstain Pattern Analysis in Crime Scenarios. Singapore: Springer Singapore, 2020.

15. Hołowko E, Januszkiewicz K, Bolewicki P, Sitnik R, Michoński J. Application of multi-resolution 3D techniques in crime scene documentation with bloodstain pattern analysis. Forensic Sci Int 2016;267:218–27.

16. Illes M, Boué M. Robust estimation for area of origin in bloodstain pattern analysis via directional analysis. Forensic Sci Int 2013;226(1–3):223–9.

17. Attinger D, Liu Y, Bybee T, De Brabanter K. A data set of bloodstain patterns for teaching and research in bloodstain pattern analysis: Impact beating spatters. Data Brief 2018;18:648–54.

18. Hakim N, Liscio E. Calculating Point of Origin of Blood Spatter Using Laser Scanning Technology. J Forensic Sci 2015;60(2):409–17.

19. Bloodstains. http://www.crimescene-forensics.com/Crime_Scene_Forensics/Bloodstains.html

20. Shen AR, Brostow GJ, Cipolla R. Toward automatic blood spatter analysis in crime scenes. IET Conference on Crime and Security. London, UK: IEE, 2006;378–83.

21. Kabaliuk N, Jermy MC, Williams E, Laber TL, Taylor MC. Experimental validation of a numerical model for predicting the trajectory of blood drops in typical crime scene conditions, including droplet deformation and breakup, with a study of the effect of indoor air currents and wind on typical spatter drop trajectories. Forensic Sci Int 2014;245:107–20.

22. Lee R, Liscio E. The accuracy of laser scanning technology on the determination of bloodstain origin. Can Soc Forensic Sci J 2016;49(1):38–51.

23. Liscio E, Hayden A, Moody J. A Comparison of the Terrestrial Laser Scanner & Total Station for Scene Documentation. :8.

24. Connolly C, Illes M, Fraser J. Affect of impact angle variations on area of origin determination in bloodstain pattern analysis. Forensic Sci Int 2012;223(1–3):233–40.

25. Liscio E. A Preliminary Validation for the FARO Zone 3D Area of Origin Tool. :10.

26. Esaias O, Noonan GW, Everist S, Roberts M, Thompson C, Krosch MN. Improved Area of Origin Estimation for Bloodstain Pattern Analysis Using 3D Scanning. J Forensic Sci 2020;65(3):722–8.

27. Camana F. Determining the area of convergence in Bloodstain Pattern Analysis: A probabilistic approach. Forensic Sci Int 2013;231(1–3):131–6.

28. Arthur RM, Hoogenboom J, Baiker M, Taylor MC, de Bruin KG. An automated approach to the classification of impact spatter and cast-off bloodstain patterns. Forensic Sci Int 2018;289:310–9.

29. Dustin D, Liscio E, Eng P. Accuracy and Repeatability of the Laser Scanner and Total Station for Crime and Accident Scene Documentation. :12.

30. Abate D, Toschi I, Sturdy-Colls C, Remondino F. A LOW-COST PANORAMIC CAMERA FOR THE 3D DOCUMENTATION OFCONTAMINATED CRIME SCENES. Int Arch Photogramm Remote Sens Spat Inf Sci 2017;XLII-2/W8:1–8.

31. Illes MB, Carter AL, Laturnus PL, Yamashita AB. Use of the Backtrack™ Computer Program for Bloodstain Pattern Analysis of Stains from Downward-Moving Drops. Can Soc Forensic Sci J 2005;38(4):213–7.

32. Raneri D. Enhancing forensic investigation through the use of modern three-dimensional (3D) imaging technologies for crime scene reconstruction. Aust J Forensic Sci 2018;:1–11.

33. Le Q, Liscio E. A comparative study between FARO Scene and FARO Zone 3D for area of origin analysis. Forensic Sci Int 2019;301:166–73.

34. Importing, Processing, and Registering Scans - FARO® Knowledge Base. https://knowledge.faro.com/Software/FARO_SCENE/SCENE/Importing-_Processing-_and_Registering_Scans

35. Scan Registration Tutorial - FARO® Knowledge Base. https://knowledge.faro.com/Software/FARO_SCENE/SCENE/Scan_Registration_Tutorial

36. Calculating Blood Spatter Origin in SCENE - FARO® Knowledge Base. https://knowledge.faro.com/Software/FARO_SCENE/SCENE/Calculating_Blood_Spatter_Origin_in_SCENE.

37. Liscio E, Bozek P, Guryn H, Le Q. Observations and 3D Analysis of Controlled Cast-Off Stains. J Forensic Sci 2020;65(4):1128–40.

38. Santoro A. Bloodstain Pattern Analysis Workflow. Leica Geosystems; White Paper :14.